# Multi-Frequency Oscillations in Self-Excited Systems

T. Bakri[*], R. Nabergoj[†] , A. Tondl[‡]

### Abstract

A self-excited three-mass chain system is here considered. For a self-excitation of van der Pol type, the possibility of multi-frequency oscillations is investigated. Both analytical approximate solutions and numerical simulation are used. The averaging method is used to establish existence and stability of the normal modes, the two-frequency modes as well as the three-frequency oscillations solutions. We found at first that the single mode seems to prevail. However a three-frequency solution can be stabilised by adapting the system slightly. A generic bifurcation diagram is given where all the possible phase portraits are sketched. The flow turns out to be quite predictable. There is no "room" for chaos or strange attractors. This behavior is not typical for systems of coupled oscillators.

*Key words:* Self-excited vibrations, three-mass chain system, coupled oscillators, bifurcations, averaging method.

*Corresponding author:* T. Bakri

---

[*]Mathematics Institute, Utrecht University, PO Box 80.010, 3508 TA Utrecht, the Netherlands.

[†]Department of Naval Architecture, Ocean and Environmental Engineering, Via Valerio 10, I-34127 Trieste, Italy.

[‡]Zborovská 41,CZ-15000 Praha 5, Czech Republic.

# 1  Introduction

Self-excited vibrations represent an important phenomenon. Although much effort has been given to the research in this field there are still some questions to be answered.

In most self-excited systems either the equilibrium position or the steady-state is unstable and, theoretically, both single- and multi-frequency vibrations could be initiated. This can be met e.g. in structures induced by flow. In general, it does not be the vibration mode corresponding to the lowest natural frequency, although this is the most common case since the lowest vibration mode prevails in many real systems. When different vibration modes are possible, some questions arise, especially whether single- or multi-frequency vibrations will finally set up.

That the single-frequency self-excited vibration prevails has been found in the research of self-excited vibration of systems having more degrees of freedom [1]. A similar behavior was found in some rotor systems where the self-excited vibration was induced due to the action of oil bearings [2,3]. To contribute to the elucidation of this problem is the aim of this paper.
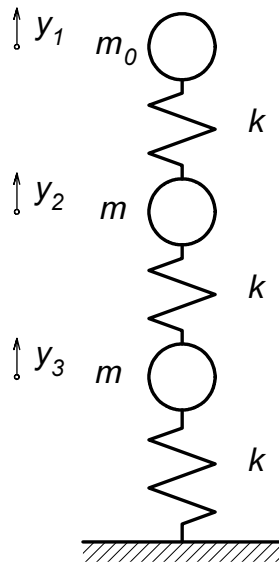


Figure 1: Schematic representation of the basic system.

## 2 Equations of motion

Let us consider a three-mass chain system the scheme of which is shown in Figure 1. Here the upper mass $m_0$, the central and lower masses $m$ represent reduced concentrated masses of structural elements while the connecting springs (having constant stiffness $k$) simulate their elasticity. Let the central and the upper masses are self-excited, e.g. by flow, which can be described by van der Pol terms. The linear viscous damping of the lower mass has coefficient $b_3$. The deflections from equilibrium positions are $y_j$ ($j = 1, 2, 3$). Thus, the considered system is governed by the following differential equations of motion:

$$\begin{cases} m_0\ddot{y}_1 - \left(b_1 - d_1y_1^2\right)\dot{y}_1 + k\left(y_1 - y_2\right) = 0 & , \\ m\ddot{y}_2 - \left(b_2 - d_2y_2^2\right)\dot{y}_2 + 2ky_2 - k\left(y_1 + y_3\right) = 0 & , \\ m\ddot{y}_3 + b_3\dot{y}_3 + ky_3 + k\left(y_3 - y_2\right) = 0 & . \end{cases} \quad (1)$$

Here $b_1$, $b_2$, $b_3$, $d_1$, $d_2$ and $k$ are positive constants. Using the time transformation $\tau = \omega_0 t$, where $\omega_0 = \sqrt{k/m}$, equations (1) get the new form:

$$\begin{cases} \ddot{y}_1 - \left(\beta_1 - \delta_1y_1^2\right)\dot{y}_1 + q^2\left(y_1 - y_2\right) = 0 & , \\ \ddot{y}_2 - \left(\beta_2 - \delta_2y_2^2\right)\dot{y}_2 + 2y_2 - \left(y_1 + y_3\right) = 0 & , \\ \ddot{y}_3 + \kappa\dot{y}_3 + 2y_3 - y_2 = 0 & , \end{cases} \quad (2)$$

where $q^2 = k/m_0\omega_0^2 = m/m_0$, $\kappa = b_3/m\omega_0$, $\beta_1 = b_1/m_0\omega_0$, $\beta_2 = b_2/m\omega_0$, $\delta_1 = d_1/m_0\omega_0$ and $\delta_2 = d_2/m\omega_0$, respectively. For sake of simplicity, the usual notation for time and time derivatives has been maintained in equation (2), as well as in further analysis.

In order to simply solve the characteristic equation of system (2):

$$\begin{vmatrix} q^2 - \Omega^2 & -q^2 & 0 \\ -1 & 2 - \Omega^2 & -1 \\ 0 & -1 & 2 - \Omega^2 \end{vmatrix} = \left(q^2 - \Omega^2\right)\left[\left(2 - \Omega^2\right)^2 - 1\right] - q^2\left(2 - \Omega^2\right) \quad , \quad (3)$$

we assume $m_0 = m/2$, and thus $q^2 = 2$. The resulting normal-mode frequencies are:

$$\begin{cases} \Omega_1 = \sqrt{2 - \sqrt{3}} \simeq 0.5176 & , \\ \Omega_2 = \sqrt{2} \simeq 1.4142 & , \\ \Omega_3 = \sqrt{2 + \sqrt{3}} \simeq 1.9319 & . \end{cases} \quad (4)$$

Equations (2) can be transformed into quasi-normal form using the linear transformation:

$$\begin{cases} y_1 = x_1 + x_2 + x_3 & , \\ y_2 = \frac{\sqrt{3}}{2}x_1 - \frac{\sqrt{3}}{2}x_3 & , \\ y_3 = \frac{1}{2}x_1 - x_2 + \frac{1}{2}x_3 & . \end{cases} \quad (5)$$

After some mathematical manipulation, required by the insertion of (5) in (2), the following system of three coupled quasi-normal equations are obtained:

$$
\begin{cases}
\ddot{x}_1 + \Omega_1^2 x_1 - \frac{1}{3}\left[\beta_1 - \delta_1\left(x_1 + x_2 + x_3\right)^2\right]\left(\dot{x}_1 + \dot{x}_2 + \dot{x}_3\right) \\
\qquad - \frac{1}{2}\left[\beta_2 - \frac{3}{4}\delta_2\left(x_1 - x_3\right)^2\right]\left(\dot{x}_1 - \dot{x}_3\right) + \frac{1}{3}\kappa\left(\frac{1}{2}\dot{x}_1 - \dot{x}_2 + \frac{1}{2}\dot{x}_3\right) = 0 \quad , \\
\ddot{x}_2 + \Omega_2^2 x_2 - \frac{1}{3}\left[\beta_1 - \delta_1\left(x_1 + x_2 + x_3\right)^2\right]\left(\dot{x}_1 + \dot{x}_2 + \dot{x}_3\right) \\
\qquad - \frac{2}{3}\kappa\left(\frac{1}{2}\dot{x}_1 - \dot{x}_2 + \frac{1}{2}\dot{x}_3\right) = 0 \quad , \\
\ddot{x}_3 + \Omega_3^2 x_3 - \frac{1}{3}\left[\beta_1 - \delta_1\left(x_1 + x_2 + x_3\right)^2\right]\left(\dot{x}_1 + \dot{x}_2 + \dot{x}_3\right) \\
\qquad + \frac{1}{2}\left[\beta_2 - \frac{3}{4}\delta_2\left(x_1 - x_3\right)^2\right]\left(\dot{x}_1 - \dot{x}_3\right) + \frac{1}{3}\kappa\left(\frac{1}{2}x_1' - \dot{x}_2 + \frac{1}{2}\dot{x}_3\right) = 0 \quad .
\end{cases}
\tag{6}
$$

For the possibility of initiation of self-excited vibration which corresponds to $j$-th natural frequency $\Omega_j$ the value of the coefficient $\Theta_{jj}$ at $\dot{x}_j$ in the $j$-th equation is decisive. For the considered system the following expressions are obtained:

$$
\begin{cases}
\Theta_{11} = \Theta_{33} = -\frac{1}{3}\beta_1 - \frac{1}{2}\beta_2 + \frac{1}{6}\kappa \quad , \\
\Theta_{22} = -\frac{1}{3}\beta_1 + \frac{2}{3}\kappa \quad .
\end{cases}
\tag{7}
$$

It is evident that, when increasing $\beta_1$ and $\beta_2$ from zero value, then $\Theta_{11}$ and $\Theta_{33}$ first reach negative values. Let us first consider the simple case $\Theta_{11} = \Theta_{33} < 0$ and $\Theta_{22} > 0$ then the case $\Theta_{11} = \Theta_{33} < 0$ and $\Theta_{22} < 0$ .

## 3    Analytical approximations

We look for the approximate solution of the autonomous system of differential equations (6), which we are going to study using the normal form method of averaging. For this purpose we introduce a scaling factor $\sqrt{\varepsilon}$ ($\varepsilon$ is a small, positive parameter) and apply the phase-amplitude transformation. The next steps are the usual ones in averaging approximations, see for instance [5]. We have:

$$
\begin{cases}
x_1(t) = R_1(t)\cos(\Omega_1 t + \phi_1(t)) \quad , \\
x_2(t) = R_2(t)\cos(\Omega_2 t + \phi_2(t)) \quad , \\
x_3(t) = R_3(t)\cos(\Omega_3 t + \phi_3(t)) \quad ,
\end{cases}
\tag{8}
$$

and

$$
\begin{cases}
\dot{x}_1(t) = -R_1(t)\Omega_1 \sin(\Omega_1 t + \phi_1(t)) \quad , \\
\dot{x}_2(t) = -R_2(t)\Omega_2 \sin(\Omega_2 t + \phi_2(t)) \quad , \\
\dot{x}_3(t) = -R_3(t)\Omega_3 \sin(\Omega_3 t + \phi_3(t)) \quad .
\end{cases}
\tag{9}
$$

After substituting (8), (9) in (6) and averaging, one yields the following:

$$
\begin{cases}
\dot{R}_1 = \varepsilon R_1 \left( -\frac{1}{2}\Theta_{11} - AR_1^2 - BR_2^2 - 2AR_3^2 \right) + O(\varepsilon^2) \quad, \\
\dot{R}_2 = \varepsilon R_2 \left( -\frac{1}{2}\Theta_{22} - BR_1^2 - \frac{1}{2}BR_2^2 - BR_3^2 \right) + O(\varepsilon^2) \quad, \\
\dot{R}_3 = \varepsilon R_3 \left( -\frac{1}{2}\Theta_{11} - 2AR_1^2 - BR_2^2 - AR_3^2 \right) + O(\varepsilon^2) \quad, \\
\dot{\phi}_i = 0 \quad, \qquad i = 1, 2, 3
\end{cases}
\tag{10}
$$

where

$$
A = \frac{B}{2} + \frac{3\delta_2}{64} > 0 \quad,
$$
$$
B = \frac{\delta_1}{12} > 0 \quad.
\tag{11}
$$

Looking for nontrivial solutions of (10), one obtains the possible combinations of normal modes. We shall in what follows distinguish between two cases.

## 3.1 The case $\Theta_{11} = \Theta_{33} < 0$ and $\Theta_{22} > 0$

From the second equation we see that assuming the second mode is nontrivial (i.e. $R_2 \neq 0$) yields the following constraint:

$$
R_1^2 + \frac{R_2^2}{2} + R_3^2 = \frac{2\beta_1 - 4\kappa}{\delta_1} = \frac{-\Theta_{22}}{2B} \quad.
\tag{12}
$$

Thus in case $\Theta_{22} > 0$ the second mode cannot exist ($R_2 = 0$). So, from looking for nontrivial equilibria of system (10), it follows that there can be two different types of solutions:

- Single-frequency solutions with the following amplitudes:

$$
\begin{cases}
R_1 = R_2 = 0 \quad, \qquad R_3 = \sqrt{-\dfrac{\Theta_{11}}{2A}} \quad, \qquad \text{or} \\
R_1 = \sqrt{-\dfrac{\Theta_{11}}{2A}} \quad, \qquad R_2 = R_3 = 0 \quad.
\end{cases}
\tag{13}
$$

  The eigenvalues of these two single-frequency solutions are the same and equal to:

$$
\lambda_1 = \Theta_{11} \quad, \qquad \lambda_2 = \frac{\Theta_{11}}{2} \quad, \qquad \text{and } \lambda_3 = -\frac{\Theta_{22}}{2} + \frac{B}{2A}\Theta_{11} \quad.
\tag{14}
$$

  Under the assumption that $\Theta_{11} = \Theta_{33} < 0$ and $\Theta_{22} > 0$, we see that the single-frequency solutions are asymptotically stable.

- One two-frequency solution with the following amplitudes:

$$
R_1 = R_3 = \sqrt{-\frac{\Theta_{11}}{6A}} \quad, \qquad R_2 = 0 \quad.
\tag{15}
$$

5

While there are no particular remarks on single-frequency vibrations, we shall now focus our attention on the existence of two-frequency vibrations. Thus, to study the stability of the two-frequency solution we linearise system (10) around the two-frequency solution. After a translation of the origin to this solution, the linearised system becomes:

$$\frac{d}{dt}\begin{pmatrix} R_1 \\ R_2 \\ R_3 \end{pmatrix} = \varepsilon C \begin{pmatrix} R_1 \\ R_2 \\ R_3 \end{pmatrix} \quad , \tag{16}$$

where:

$$C = \begin{pmatrix} \dfrac{\Theta_{11}}{3} & 0 & \dfrac{2\Theta_{11}}{3} \\ 0 & -\dfrac{\Theta_{22}}{2} + \dfrac{B}{3A}\Theta_{11} & 0 \\ \dfrac{2\Theta_{11}}{3} & 0 & \dfrac{\Theta_{11}}{3} \end{pmatrix} \quad . \tag{17}$$

We obtain for the eigenvalues $\lambda_i$ of the matrix $C$ the following expressions:

$$\begin{cases} \lambda_1 = -\dfrac{\Theta_{11}}{3} > 0 \quad , \\ \lambda_2 = \Theta_{11} < 0 \quad , \\ \lambda_3 = -\dfrac{\Theta_{22}}{2} + \dfrac{B}{3A}\Theta_{11} \quad . \end{cases} \tag{18}$$

One comes to the conclusion that the two-frequency solution is, when it exists, always unstable no matter what the parameters are since one of the eigenvalues is positive. This confirms the fact that in most real systems the single-frequency self-excited vibration prevails [1]. In other words, it is very difficult to spot this solution numerically as it has a saddle character.

## 3.2 The case $\Theta_{11} = \Theta_{33} < 0$ and $\Theta_{22} < 0$

Applying the same approach as in the previous case, we find the following types of solutions:

- Three single-frequency solutions with the following amplitudes and stability:

  - $R_1 = \sqrt{-\dfrac{\Theta_{11}}{2A}}$, $R_2 = R_3 = 0$, with eigenvalues

$$\lambda_1 = \Theta_{11} \ , \ \ \lambda_2 = -\frac{\Theta_{22}}{2} + \frac{B}{2A}\Theta_{11} \text{ and } \lambda_3 = \frac{\Theta_{11}}{2} \ . \tag{19}$$

  - $R_3 = \sqrt{-\dfrac{\Theta_{11}}{2A}}$, $R_1 = R_2 = 0$, with eigenvalues

$$\lambda_1 = \Theta_{11} \ , \ \ \lambda_2 = -\frac{\Theta_{22}}{2} + \frac{B}{2A}\Theta_{11} \text{ and } \lambda_3 = \frac{\Theta_{11}}{2} \ . \tag{20}$$

  - $R_2 = \sqrt{-\dfrac{\Theta_{22}}{B}}$, $R_2 = R_3 = 0$, with eigenvalues

$$\lambda_1 = \Theta_{22} \ , \ \ \lambda_2 = \lambda_3 = \Theta_{22} - \frac{\Theta_{11}}{2} \ . \tag{21}$$

  We see that the first and the third single mode solutions are asymptotically stable if

$$\frac{B}{2A}\Theta_{11} - \frac{\Theta_{22}}{2} < 0 \quad , \tag{22}$$

  while the second mode is asymptotically stable if

$$\Theta_{22} - \frac{\Theta_{11}}{2} < 0 \quad . \tag{23}$$

- Three two-frequency solutions with the following amplitudes and stability:

  - $R_2 = 0$, $R_1 = R_3 = \sqrt{-\dfrac{\Theta_{11}}{6A}}$. $\tag{24}$

  From the previous section, we see that this solution is always unstable as $\Theta_{11} = \Theta_{33} < 0$.

  - $R_1 = 0$, $R_3 = \sqrt{\dfrac{\Theta_{22} - \Theta_{11}/2}{A - 2B}}$, $R_2 = \sqrt{\dfrac{\Theta_{11} - A\Theta_{22}/B}{A - 2B}}$. $\tag{25}$

  - $R_3 = 0$, $R_1 = \sqrt{\dfrac{\Theta_{22} - \Theta_{11}/2}{A - 2B}}$, $R_2 = \sqrt{\dfrac{\Theta_{11} - A\Theta_{22}/B}{A - 2B}}$. $\tag{26}$

  Analysis of the eigenvalues yield that these two solution exist and are unstable if

$$\Theta_{22} - \frac{\Theta_{11}}{2} < 0 \ \text{ and } A - 2B < 0 \ , \tag{27}$$

  and asymptotically stable if

$$\Theta_{22} - \frac{\Theta_{11}}{2} > 0 \ \text{ and } A - 2B > 0 \ . \tag{28}$$

- One unstable three-frequency solution with the following amplitudes:

$$R_2 = \sqrt{\frac{2\Theta_{11} - 3A\Theta_{22}/B}{3A - 4B}} \ , \ \ R_1 = R_3 = \sqrt{\frac{\Theta_{22} - \Theta_{11}/2}{3A - 4B}} \ . \tag{29}$$

7

## 3.3 Results

Under the assumption $\Theta_{11} = \Theta_{33} < 0$ and $\Theta_{22} < 0$ we found two asymptotically stable two-frequency solutions, see Figure 2. The region in the parameter space where the two-frequency solution is stable is small, as we shall see in Figure 4, region ⓑ below, but has measure bigger than zero. So it is likely to hit this set by chance. In spite of the three oscillators being self-excited in this case, the three-frequency solution does not prevail as it is always of the saddle type. Now that enough is known about the stability of these modes, we shall proceed by giving the generic bifurcation diagram.
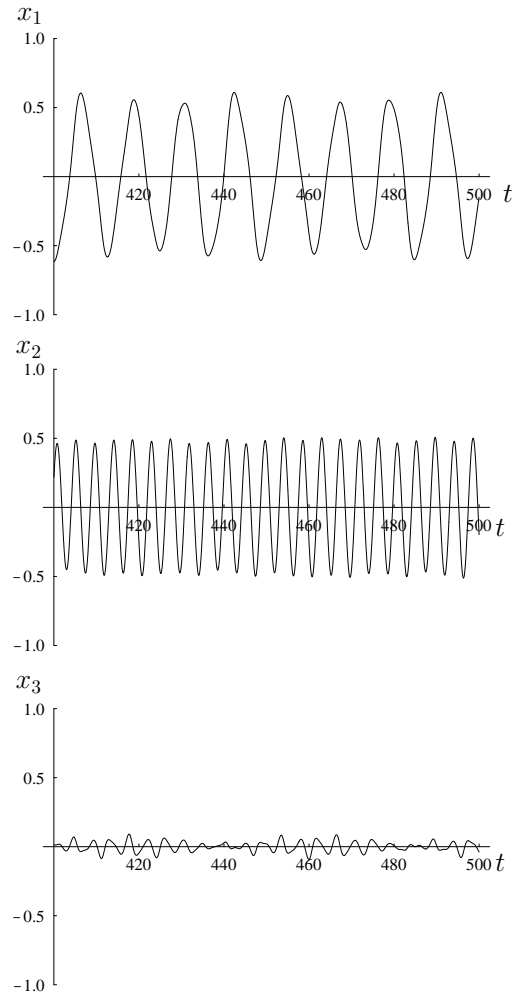


Figure 2: Vibration records of $x_1$, $x_2$ and $x_3$ corresponding to system (6) as a function of time with $\beta_1 = 0.3$; $\beta_2 = 0.15$; $\delta_1 = 0.5$; $\delta_2 = 4.0$; $\kappa = 0.1$; $x_1(0) = 1.818$; $x_2(0) = 0.997$; $x_3(0) = 0.589$; $\dot{x}_1(0) = \dot{x}_2(0) = \dot{x}_3(0) = 0$ showing the presence of a stable two-frequency solution.

# 4  Bifurcation diagrams

For details on the bifurcation diagram in the two-dimensional case, we refer to [4], see in chapter 8 the section on Hopf-Hopf bifurcation. Here, more or less the same notation as in [4] will be adopted.

First we mention that system (10) has four invariant manifolds, namely:

$$
\begin{aligned}
M_1 &= \left\{(R_1, R_2, R_3) \in \mathbb{R}^3 : \ R_1 = 0\right\} \quad , \\
M_2 &= \left\{(R_1, R_2, R_3) \in \mathbb{R}^3 : \ R_2 = 0\right\} \quad , \\
M_3 &= \left\{(R_1, R_2, R_3) \in \mathbb{R}^3 : \ R_3 = 0\right\} \quad , \\
M_4 &= \left\{(R_1, R_2, R_3) \in \mathbb{R}^3 : \ R_1 = R_3\right\} \quad .
\end{aligned}
\tag{30}
$$

$M_4$ is an unstable invariant manifold acting as a separatrix. If we start in the region enclosed by $M_2$, $M_1$ and $M_4$, the flow will evolve towards the invariant manifold $M_1$. If on the other hand we start in the region enclosed by the manifolds $M_2$, $M_3$ and $M_4$, the flow will evolve towards the invariant manifold $M_3$. It is therefore sufficient to give the bifurcation diagram on these four manifolds to completely understand the dynamics. In what follows, we shall refer to the $i-$th normal mode by $P_i$, $i = 1, 2, 3$, whereas $P_{ij}$ denotes the two-frequency solution where only the $i-$th and the $j-$th component oscillate, the third mode being at rest. Accordingly, $P_{123}$ denotes the 3-mode solution. The case $\Theta_{11} = \Theta_{33} < 0$, $\Theta_{22} > 0$ as well as the case $\Theta_{11} = \Theta_{33} > 0$, $\Theta_{22} > 0$ are quite straightforward. They yield a rather trivial bifurcation diagram. We therefore focus in the sequel on the case $\Theta_{11} = \Theta_{33} < 0$, $\Theta_{22} < 0$.

One sees from equation (26) that the nontrivial equilibrium $P_{12}$ collides respectively with $P_2$ and $P_3$ and disappears on the bifurcations curves:

$$
D_1 = \left\{(\Theta_{11}, \Theta_{22}) : \ \Theta_{22} = \frac{1}{2}\Theta_{11}, \ \Theta_{11} = \Theta_{33} < 0\right\} \quad ,
\tag{31}
$$

and

$$
D_2 = \left\{(\Theta_{11}, \Theta_{22}) : \ \Theta_{22} = \frac{B}{A}\,\Theta_{11}, \ \Theta_{11} = \Theta_{33} < 0\right\}.
\tag{32}
$$

On the other hand, equation (25) shows that the nontrivial equilibrium $P_{23}$ collides respectively with $P_2$ and $P_1$ on the bifurcation curves $D_1$ and $D_2$. Finally, it follows from equation (29) that the nontrivial equilibrium $P_{123}$ collides with $P_2$ and disappears on the bifurca-

tion curve $D_1$. It also collides with $P_{13}$ and disappears on the bifurcation curve:

$$D_3 = \left\{ (\Theta_{11}, \Theta_{22}) : \; \Theta_{22} = \frac{2B}{3A} \Theta_{11}, \; \Theta_{11} = \Theta_{33} < 0 \right\}.$$ (33)

The following three topologically different bifurcation diagrams are all one can encounter in this system under the assumption made on the parameters:

1. $\dfrac{B}{A} < \dfrac{1}{2}$ ,

2. $\dfrac{1}{2} < \dfrac{B}{A} < \dfrac{3}{4}$ ,

3. $\dfrac{3}{4} < \dfrac{B}{A} < 2$ .

In all the three cases the flow on the invariant manifold $M_2$ is the same. We shall therefore for the sake of brevity omit it from the figure with the generic phase portraits, but give it once in Figure 3. In the drawing we show the approximate solutions $R_1$ and $R_3$ of equation (10) for $R_2 = 0$. The strait line through the origin and the saddle multi-frequency solution $P_{13}$ is a separatrix. It divides the $R_1 R_3$ plane into two domains of attraction. Starting in the domain between the $R_1$-axis and the separatrix, the orbits will converge to the single-frequency solution $P_1$ corresponding to vibrations with frequency $\Omega_1$. Starting on the other hand in the complementary domain, the orbits converge to the single-frequency solution $P_3$ corresponding to vibrations with frequency $\Omega_3$. In other words, outside the separatrix, only single vibrations can occur in the $R_1 R_2$ plane.
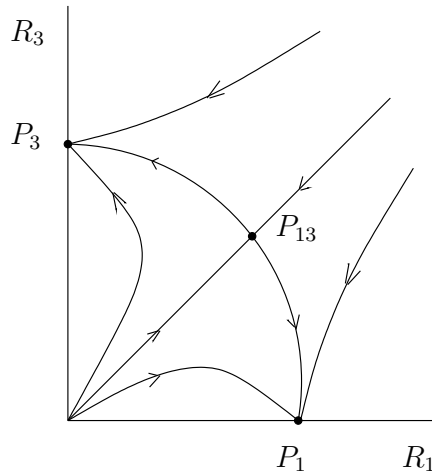


Figure 3: Generic phase portrait on the invariant manifold $M_2$, i.e., $R_2 = 0$.

10

The $(\Theta_{11}, \Theta_{22})$ parametric portraits corresponding to the cases 1–3 are shown in Figure 4, while the only possible generic phase portraits are given in Figure 5. In Figure 5 each of the different types of phase portraits ⓐ–ⓕ is given as a collection of the three portraits on the invariant manifolds $M_1$, $M_3$ and $M_4$ which define, as we stated above, completely the flow. If we take for instance type ⓐ we see that in this case the second mode $P_2$ is the only stable solution the system has, so we will always end up at $P_2$ when doing numerical simulations. Case ⓑ shows the presence of a three-mode $P_{123}$ which looks stable; however as it lies in the unstable manifold $M_4$ it is therefore unstable. We have in this case two stable two-frequency modes namely, $P_{23}$ and $P_{12}$. The single modes are all unstable. So combining the Figures 2 and 3 one can draw out the type of flow there is given the parameters of the system. We see that the dynamics is quite simple in the sense that the flow behaves, under all circumstances, in a predictable manner. There are no "exotic" bifurcations nor chaotic regions in the parameter space.
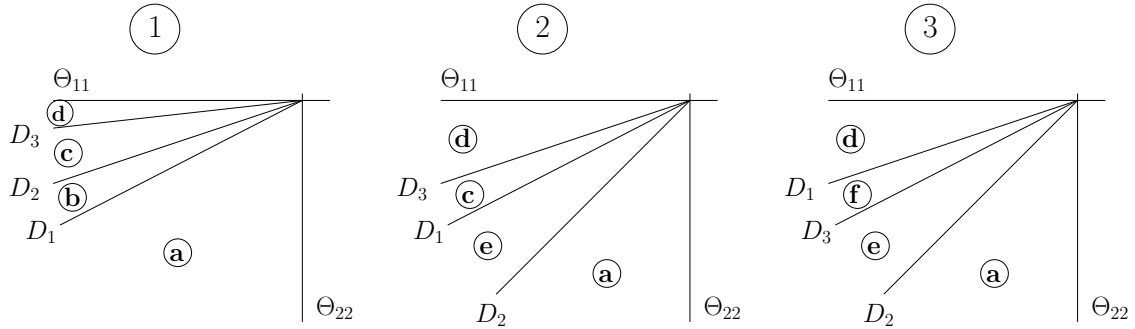


Figure 4: $(\Theta_{11}, \Theta_{22})$ parametric portraits corresponding to system (10).

11
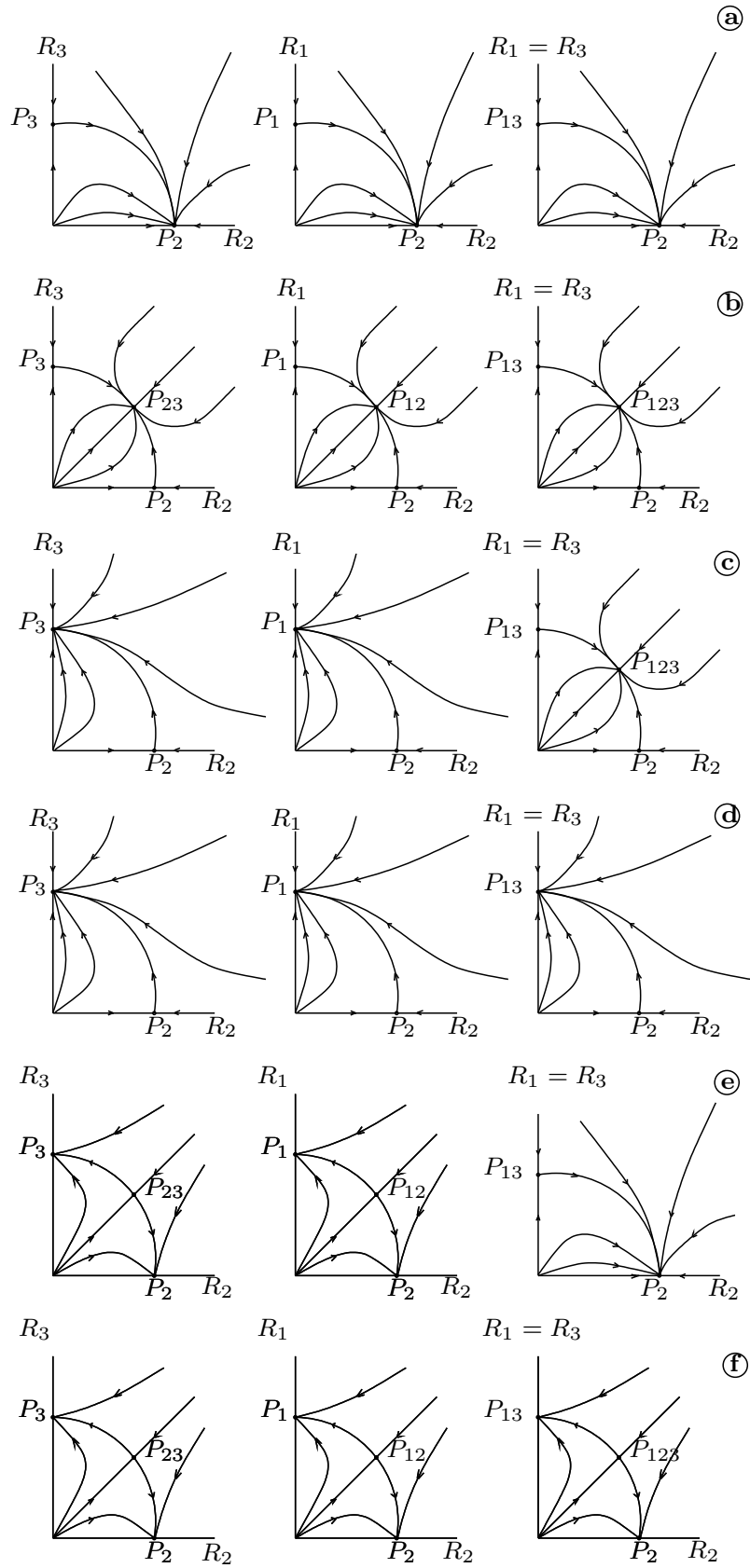
Figure 5: Generic phase portraits of system (10).

# 5  A system with a stable multi-frequency vibration

Although the spirit of this paper is to stress that single-frequency solutions often prevail, in the following example we show that this is not always the case. We adapt system (6) by adding quadratic terms and scaling in the following manner: $x_i = \sqrt{\varepsilon}\overline{x}_i$, $\beta_i = \varepsilon\overline{\beta}_i$, $\kappa = \varepsilon\overline{\kappa}$, $a = \sqrt{\varepsilon}\overline{a}$. Omitting the bars yields:

$$
\begin{cases}
\ddot{x}_1 + \Omega_1^2 x_1 - \frac{1}{3}\varepsilon\left[\beta_1 - \delta_1(x_1 + x_2 + x_3)^2\right](\dot{x}_1 + \dot{x}_2 + \dot{x}_3) \\
\qquad -\frac{1}{2}\varepsilon\left[\beta_2 - \frac{3}{4}\delta_2(x_1 - x_3)^2\right](\dot{x}_1 - \dot{x}_3) + \frac{1}{3}\varepsilon\kappa\left(\frac{1}{2}\dot{x}_1 - \dot{x}_2 + \frac{1}{2}\dot{x}_3\right) - \varepsilon a\dot{x}_3 x_2 = 0 \quad, \\
\ddot{x}_2 + \Omega_2^2 x_2 - \frac{1}{3}\varepsilon\left[\beta_1 - \delta_1(x_1 + x_2 + x_3)^2\right](\dot{x}_1 + \dot{x}_2 + \dot{x}_3) \\
\qquad -\frac{2}{3}\varepsilon\kappa\left(\frac{1}{2}\dot{x}_1 - \dot{x}_2 + \frac{1}{2}\dot{x}_3\right) - \varepsilon a\dot{x}_3 x_1 = 0 \quad, \\
\ddot{x}_3 + \Omega_3^2 x_3 - \frac{1}{3}\varepsilon\left[\beta_1 - \delta_1(x_1 + x_2 + x_3)^2\right](\dot{x}_1 + \dot{x}_2 + \dot{x}_3) \\
\qquad +\frac{1}{2}\varepsilon\left[\beta_2 - \frac{3}{4}\delta_2(x_1 - x_3)^2\right](\dot{x}_1 - \dot{x}_3) + \frac{1}{3}\varepsilon\kappa\left(\frac{1}{2}\dot{x}_1 - \dot{x}_2 + \frac{1}{2}\dot{x}_3\right) - \varepsilon a\dot{x}_2 x_1 = 0 \quad.
\end{cases}
\tag{34}
$$

This system has under certain circumstances a stable 3-mode, see Figure 6. We can show this result by averaging the system and studying the averaged flow.

Averaging system (34) and reducing the dimension yields:

$$
\begin{cases}
\dot{R}_1 = \varepsilon R_1\left(-\frac{1}{2}\Theta_{11} - AR_1^2 - BR_2^2 - 2AR_3^2\right) + \varepsilon\dfrac{a\Omega_3}{4\Omega_1}R_2 R_3\cos\theta \quad, \\[2mm]
\dot{R}_2 = \varepsilon R_2\left(-\frac{1}{2}\Theta_{22} - BR_1^2 - \frac{1}{2}BR_2^2 - BR_3^2\right) + \varepsilon\dfrac{a\Omega_3}{4\Omega_2}R_1 R_3\cos\theta \quad, \\[2mm]
\dot{R}_3 = \varepsilon R_3\left(-\frac{1}{2}\Theta_{11} - 2AR_1^2 - BR_2^2 - AR_3^2\right) + \varepsilon\dfrac{a\Omega_2}{4\Omega_3}R_1 R_2\cos\theta \quad, \\[2mm]
\dot{\theta} = \frac{1}{4}\varepsilon a\sin\theta\left(\dfrac{R_1 R_2}{R_3}\dfrac{\Omega_2}{\Omega_3} - \dfrac{R_1 R_3}{R_2}\dfrac{\Omega_3}{\Omega_2} - \dfrac{R_2 R_3}{R_1}\dfrac{\Omega_3}{\Omega_1}\right) \quad,
\end{cases}
\tag{35}
$$

where $\theta(t) = \phi_3(t) - \phi_2(t) - \phi_1(t)$. Setting the right-hand side of (35) equal to zero yields a system of equations, which unfortunately cannot be solved explicitly. The roots can however be computed numerically quite easily.

## 5.1  Results of numerical simulation

The differential equations of motion (34) have been used for numerical simulation. For the sake of comparison with theoretical predictions the quasi-normal deflections $x_j$ $(j = 1, 2, 3)$ have been considered. The following parameter values were used in our numerical analysis: $a = 4$, $\beta_1 = \beta_2 = 1.5$, $\delta_1 = \delta_2 = 4$, $\varepsilon = 0.01$, $\kappa = 1$.

The averaging method gives the first order approximation of the amplitudes $R_1$, $R_2$ and $R_3$ of the stable 3-mode solution. For the parameter values under consideration we found $R_1 = 1.81788$, $R_2 = 0.997464$, $R_3 = 0.588998$. The results are summarised in Figure 6.
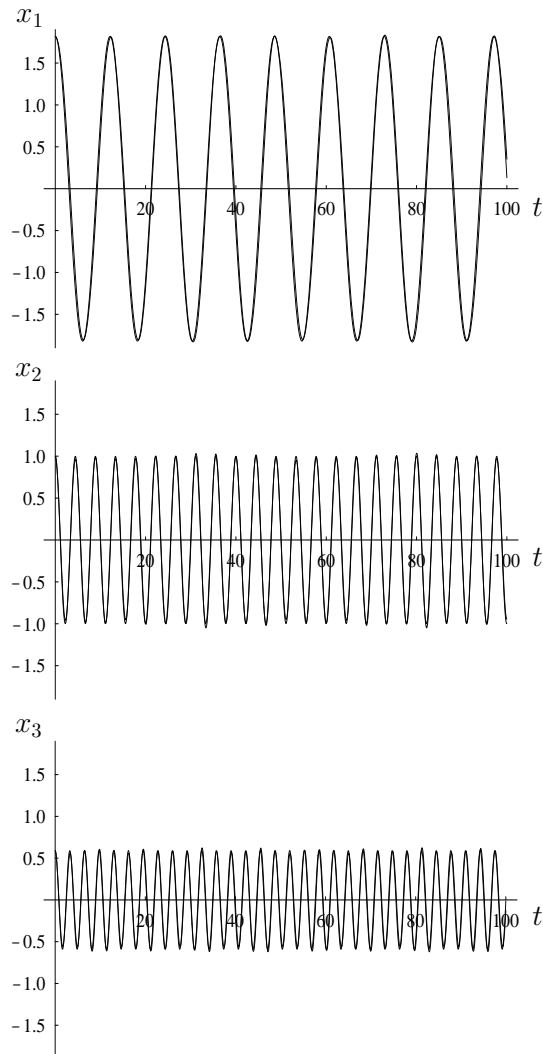


Figure 6: Superposition of the vibration records of $x_1(t)$, $x_2(t)$ and $x_3(t)$, corresponding to system (34), with $x_1(0) = 1.818$; $x_2(0) = 0.997$; $x_3(0) = 0.589$; $\dot{x}_1(0) = \dot{x}_2(0) = \dot{x}_3(0) = 0$ and their corresponding normal modes $R_i \cos \Omega_i t$ for $t \in [0, 100]$.

The superposition of the averaged solution and the exact solution is here shown only for a time scale of order $1/\varepsilon$. As we can see there is very good agreement between the averaging method and the numerical simulation. After that time limit the shift in the phase becomes too important and the averaged solution slowly drifts off from the exact solution as expected,

see Figure 7. The amplitudes however remain the same. This was expected as well.
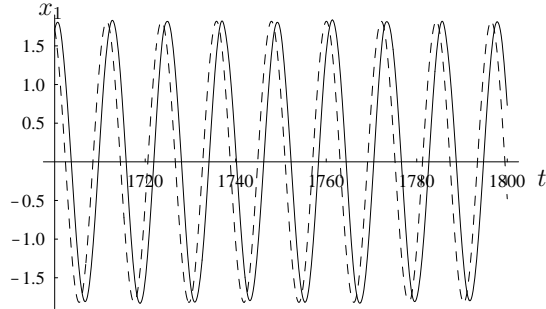


Figure 7: The averaging solution corresponding with the first mode $x_1(t)$ (dashed line) drifts off from the exact solution (full line) for higher values of the time $t > O(1/\varepsilon)$.

## 5.2   Bifurcation analysis

We shall in the sequel restrict the bifurcation study to the case of self-excitation of the first and the third component only, i.e., $\Theta_{22} > 0$, $\Theta_{11} = \Theta_{33} < 0$.

Starting at the parameter value $a = 0$ we continue all the possible modes found in the averaged system with respect to the parameter $a$ and see which bifurcations do take place. The results, which also hold for the original system (34), are summarised in Figure 8. At $a = 0$, the normal modes are: $P_1 = 1.236694 \cos \Omega_1 t$, $P_3 = 1.236694 \cos \Omega_3 t$, and $P_{13} = 0.714 \cos \Omega_1 t + 0.714 \cos \Omega_3 t$.

In this investigation we continued the unstable 2-mode $P_{13}$ with respect to the parameter $a$. When $a$ increases, the unstable 2-mode becomes an unstable 3-mode which evolves according to the dotted line. At the parameter value $a_{c_1} = 0.81$ it coalesces with the stable single mode $P_3$ creating a branching point and then disappears. When $a = 0$, $P_3$, is asymptotically stable. Beyond the branching point value $a_{c_1} = 0.81$, this mode continues to exist but becomes unstable.

The single mode $P_1$ remains stable as $a$ grows form 0 to $a_{c_2} = 1.83$. At this critical value a stable 3-mode emerges from $P_1$ creating a second branching point and making $P_1$ unstable. The stable 3-mode evolves according to the full line as $a$ increases. No other bifurcations or interesting phenomena were observed as $a$ increased further. Also no other significant behaviour occurs if we continue these modes with respect to other parameters.
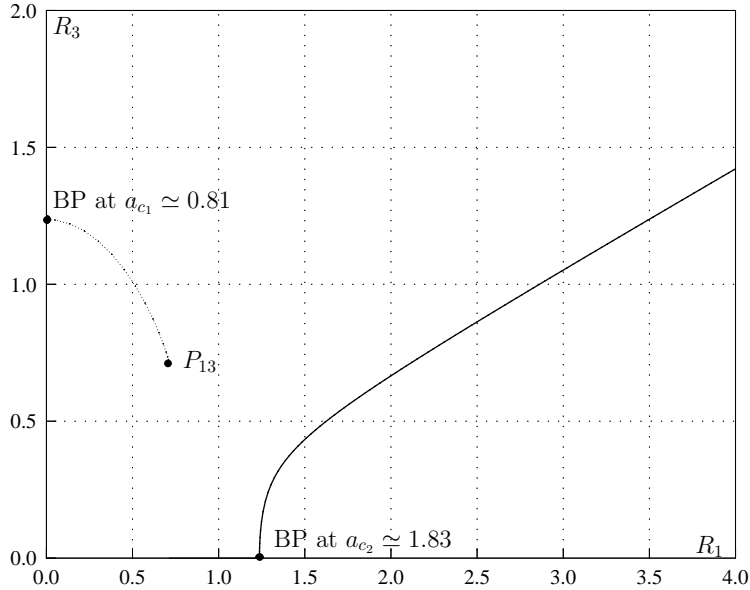
Figure 8: Bifurcation diagram of the possible modes, projected onto the $R_1 R_3$ – plane, with respect to the parameter $a$. BP stands for Branching Point bifurcation.

## 5.3 Remarks

The modes $P_{13}$ and $P_{123}$ correspond to quasi-periodic motion in the original system. The birth of these tori is due to these branching points. This is in averaging a complete different scenario from the Neimark-Sacker bifurcation, where we also have a birth of a torus, but in this case the second period of the torus is always $O(1/\varepsilon)$ whereas in our system the second (and third period in the case of $P_{123}$) are $O(1)$.

The critical values $a_{c_1}$ and $a_{c_2}$ can be computed exactly by monitoring the eigenvalues of the system obtained by linearising system (35) around $P_3$ and $P_1$ respectively. At the branching point bifurcation, one of the eigenvalues becomes zero. We find:

$$a_{c_2} = 2\sqrt{2}\sqrt{A\Theta_{22} - B\Theta_{11}} \quad , \tag{36}$$

$$a_{c_1} = \sqrt{3\sqrt{3} - 5}\, a_{c_2} \quad . \tag{37}$$

# 6 Conclusion

Using the normal form method of averaging, we were able to explore the system deeply. We come, after producing the bifurcation diagram, to the conclusion that the system behaves in a quite predictable manner. No complicated dynamics like strange attractors or chaotic be-

havior were found as one would have expected. There are many examples of even two-coupled oscillators where very complicated dynamics occur including torus breakdown, strange attractors and chaos. See for example [6]. Also we were able to answer the question whether the single mode always prevails in this type of coupled oscillators. We found the two-frequency solution of the original quasi-normal self-excited system is, when it exists, always unstable no matter what the parameters are. Adding, however a specific quadratic term to the basic system (6) to obtain system (34), we were able to destabilise the single modes and stabilise a 3-mode solution leading to the conclusion that in a slightly modified system the single mode does not always prevail.

## Acknowledgment

## References

[1] Tondl, A., Self-Excited Vibrations. National Research Institute for Machine Design, Monograph and memoranda No. 9, Prague (1970).

[2] Tondl, A., Notes on the Problem of Self-Excited Vibrations and Nonlinear Resonances of Rotors Supported on Several Journal Bearings, Wear 8, 349-357 (1965).

[3] Šafr, M., private communication (2002).

[4] Yu.A. Kuznetsov, *Elements of Applied Bifurcation Theory*, 2nd Edition, Springer, New York, 1995.

[5] F. Verhulst, *Nonlinear Differential Equations and Dynamical Systems*, Springer, Berlin, Heidelberg, 1996.

[6] T. Bakri, *Torus Breakdown and Chaos in a System of Coupled Oscillators*, to be published in the International Journal of Non-Linear Mechanics.